Oxygen Exchange at the Internal Surface of Amorphous SiO_2 Studied by Photoluminescence of Isotopically Labeled Oxygen Molecules

Koichi Kajihara,[1,2,*] Taisuke Miura,[3] Hayato Kamioka,[4] Masahiro Hirano,[1,6] Linards Skuja,[1,5] and Hideo Hosono[1,6]

[1]*Transparent Electro-Active Materials Project, ERATO-SORST, Japan Science and Technology Agency, in Frontier Research Center, S2-13, Tokyo Institute of Technology, 4259 Nagatsuta, Midori-ku, Yokohama 226-8503, Japan*

[2]*Department of Applied Chemistry, Graduate School of Urban Environmental Sciences, Tokyo Metropolitan University, 1-1 Minami-Osawa, Hachioji 192-0397, Japan*

[3]*Research & Development Division, OMRON Laserfront Inc., 1120 Shimokuzawa, Sagamihara 229-1198, Japan*

[4]*Graduate School of Pure and Applied Sciences, University of Tsukuba, 1-1-1 Tennodai, Tsukuba 305-8571, Japan*

[5]*Institute of Solid State Physics, University of Latvia, Kengaraga iela 8, LV1063 Riga, Latvia*

[6]*Materials and Structures Laboratory & Frontier Research Center, Tokyo Institute of Technology, 4259 Nagatsuta, Midori-ku, Yokohama 226-8503, Japan*

(Received 12 February 2009; published 27 April 2009)

The exchange between lattice and interstitial oxygen species in an oxide was studied by the ^{16}O-^{18}O isotope shift of the $a^1\Delta_g(v=0) \rightarrow X^3\Sigma_g^-(v=1)$ infrared photoluminescence band of the oxygen molecules (O_2) incorporated into the interstitial voids of amorphous SiO_2 (a-SiO_2) by thermal annealing in $^{18}O_2$ gas. A large site to site variation of the oxygen exchange rate, originating from structural disorder of a-SiO_2, is found. The average exchange rate has an activation energy of $\sim$2 eV, which is much larger than that for the diffusion of interstitial O_2 ($\sim$0.8–1.2 eV). The average exchange-free diffusion length of interstitial O_2 exceeds $\sim 1\ \mu$m below 900 °C, providing definite evidence that oxygen diffuses as interstitial molecules in a-SiO_2.

DOI: 10.1103/PhysRevLett.102.175502 PACS numbers: 61.72.jj, 65.60.+a, 66.30.hh, 78.55.Qr

Various properties of oxides relevant to practical applications, such as electrical and ionic conductivity, optical transparency, and catalytic activity, are closely related to the oxygen transfer between the oxides themselves and ambient oxygen molecules (O_2). The interaction of O_2 with oxide surfaces has been studied extensively [1–3]. Amorphous SiO_2 (a-SiO_2) is unique among oxides due to its low density and interstitial voids which may be treated as ''internal surfaces.'' The oxygen transfer occurring at the internal surfaces between the molecules in a ''quasigas phase'' and the surrounding lattice oxygen in the a-SiO_2 network is of fundamental interest because it is intrinsic, that is, unaffected by passivated dangling bonds and adatoms covering the outer surfaces. Moreover, the diffusion of interstitial O_2 in a-SiO_2 is technologically important as it is a key step in growing dielectric a-SiO_2 films on silicon microelectronic circuits [4,5]. It is considered that interstitial O_2 diffuses without significant exchange with the surrounding a-SiO_2 network [6–10]; however, some oxygen exchange has been found to occur [11–13]. The details have remained uncertain primarily because the concentration of interstitial O_2 is several orders of magnitude smaller than that of the background oxygen network atoms, and at the time of these studies, experimental techniques that are able to distinguish interstitial O_2 from the background were absent.

Oxygen molecules dissolved in solids and liquids can be selectively detected via their characteristic infrared (IR) photoluminescence (PL) due to the transition from the first singlet excited state $a^1\Delta_g$ to the triplet ground state $X^3\Sigma_g^-$ of O_2 (pure electronic band, PEB) [14,15]. This method has been useful in the study of the diffusion and reactions of O_2 in a-SiO_2 [16–18]. We demonstrate here that the oxygen exchange between interstitial O_2 and the a-SiO_2 network is quantitatively studied by combining the PL method with an isotope labeling technique. Since the shape and peak position of PEB are insensitive to isotopic substitution [19], the isotopologues of interstitial O_2 are distinguished using the PL band due to the transition from the a state to the first vibronic level of the X state $X^3\Sigma_g^-(v=1)$ (vibrational sideband, VSB), which is much weaker than PEB but undergoes a strong isotope shift.

High-purity synthetic a-SiO_2 specimens ($10 \times 6.5 \times 0.4$–0.5 mm^3 with two optically polished faces) containing $\sim 2 \times 10^{18}$ cm^{-3} SiOH groups were sealed in an SiOH-free (SiOH $\lesssim 10^{17}$ cm^{-3}) silica tubes with $^{18}O_2$ (^{18}O isotopic purity $\gtrsim$99%) or $^{16}O_2$ gas of 0.9 atm at room temperature. The sealed silica tube, each containing eight specimens, were thermally annealed between 500 and 900 °C. Before and after the thermal annealing, the isotopic composition of O_2 gas in the silica tube was monitored by conventional Raman spectrometry [20] and was nearly unchanged [21]. The O_2-loaded samples were taken out of the tube, and the PL bands were excited at 765 nm using an AlGaAs laser diode ($\sim$1.5 W at the sample position) via the forbidden transition to the second singlet excited state $b^1\Sigma_g^+$ of interstitial O_2. Since VSB is very weak, the eight specimens were stacked to facilitate the detection. The sample stack was irradiated normal to the polished face and the backscattered PL emission was re-

corded by a Fourier-transform IR Raman spectrometer (Model 960, Nicolet). The PL time decay curves were also measured (technique is described in Ref. [22]) to evaluate the possible variation in the PL quantum yield with the isotopic substitution.

Figure 1 shows PL spectra for samples thermally annealed in $^{16}O_2$ or $^{18}O_2$. The $^{16}O_2$ loading was performed for 72 h at 700 °C, whereas the $^{18}O_2$ loading was done with a shorter time at lower temperature (12 h at 500 °C) to maximize ^{18}O fraction in interstitial O_2. The spectra were normalized to the intensity of PEB at $\sim$7855 cm^{-1} [15,23], showing a negligible shift upon ^{18}O substitution. VSB of interstitial $^{16}O_2$ PL was observed at $\nu_{66} \simeq 6308$ cm^{-1}, and the band shape was simulated well with a pseudo Voigt function. In the $^{18}O_2$-loaded sample, VSB was shifted to a higher energy side along with a $\sim$20% increase in the normalized amplitude. This band is mainly due to interstitial $^{18}O_2$ because the peak position agrees well with that expected from the atomic mass ratio between ^{16}O and ^{18}O and the PEB and VSB positions of interstitial $^{16}O_2$ ($\nu_{68} \simeq 6352$ cm^{-1} for $^{16}O^{18}O$ and $\nu_{88} \simeq 6397$ cm^{-1} for $^{18}O_2$). However, its shape was slightly asymmetric due to small amounts of $^{16}O^{18}O$ and $^{16}O_2$ formed by oxygen exchange with the a-SiO_2 network. The observed spectrum was decomposed into three VSBs of $^{16}O_2$, $^{16}O^{18}O$, and $^{18}O_2$ to evaluate the respective isotopic fractions f_{66}, f_{68}, and f_{88} ($f_{66} + f_{68} + f_{88} = 1$) as follows. The peak positions of VSBs were fixed at ν_{66}, ν_{68}, and ν_{88}. The peak amplitude and width of $^{18}O_2$ VSB as well as f_{66} and f_{88} were treated as variables. The peak amplitude and width of $^{16}O^{18}O$ VSB were assumed to be given by linear interpolations of those of $^{16}O_2$ and $^{18}O_2$ VSBs. This procedure confirmed the high ^{18}O purity ($f_{88} + f_{68}/2 \sim 0.97$) of O_2 in the $^{18}O_2$-loaded sample and determined the peak parameters of VSBs of interstitial $^{18}O_2$ and $^{16}O^{18}O$ that are needed for the following concentration analysis based on VSBs.

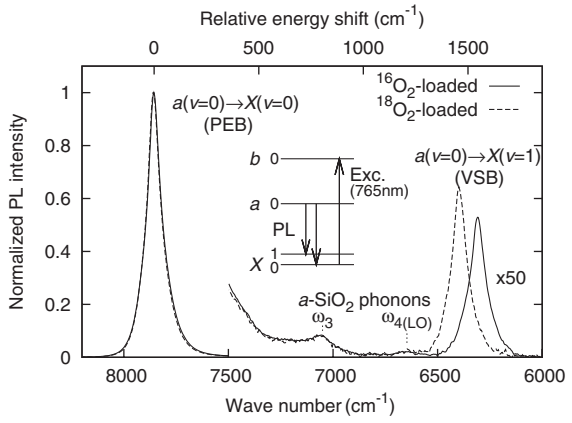

FIG. 1. PL spectra of interstitial O_2 in samples thermally annealed in $^{16}O_2$ for 72 h at 700 °C or $^{18}O_2$ for 12 h at 500 °C. Schematic diagram of interstitial O_2 energy levels is also shown. The spectra were normalized to the amplitude of the pure electronic band (PEB) at $\sim$7855 cm^{-1}. The vibrational sideband (VSB) appears at $\sim$6300–6400 cm^{-1}. Small peaks located between 6500 and 7500 cm^{-1} are due to interactions with phonons of the a-SiO_2 network.

Figure 2 shows the VSB spectra for the samples thermally annealed at 700 °C in $^{16}O_2$ or $^{18}O_2$ for up to 72 h. The spectra of the $^{18}O_2$-loaded samples clearly consisted of three VSBs of interstitial $^{16}O_2$, $^{16}O^{18}O$, and $^{18}O_2$. The ^{18}O fraction of interstitial O_2 ($f_{88} + f_{68}/2$) decreased monotonically with an increase in annealing time, confirming the transfer of ^{16}O from the a-SiO_2 network to interstitial O_2. Figure 3 summarizes variation of f_{66} and f_{88} with time and temperature of $^{18}O_2$ loading. f_{66} and f_{88} evaluated by peak decomposition of the VSB spectra are denoted as filled symbols.

The total concentration of interstitial O_2, C_T, was determined by comparing the PEB intensity with that of a reference sample of known interstitial $^{16}O_2$ concentration [18]. The PL quantum yield of PEB is proportional to the decay constant τ [22], and τ_{68} and τ_{88} were found to be $\sim$1.7 and $\sim$2.5 times larger than τ_{66}, respectively. This uneven PL quantum yield was corrected by multiplying the PEB intensity with the factor $\tau_{66}/(f_{66}\tau_{66} + f_{68}\tau_{68} + f_{88}\tau_{88})$. The O_2 concentrations evaluated with this procedure agree with those calculated from the Arrhenius relations of the solubility S and diffusion coefficient D determined from measurements above 800 °C [17,18]. Thus, the Arrhenius relations were used to produce D, S, and C_T values in the following numerical simulation of the oxygen exchange.

The exchange of an interstitial O_2 molecule with the a-SiO_2 network may be a reversible second order reaction, transferring only an oxygen atom in each exchange event [11,24],

$$^{18}O^{18}O + \equiv Si\text{-}^{16}O\text{-}Si \equiv \rightleftarrows {}^{16}O^{18}O + \equiv Si\text{-}^{18}O\text{-}Si \equiv, \quad (1)$$

$$^{16}O^{18}O + \equiv Si\text{-}^{16}O\text{-}Si \equiv \rightleftarrows {}^{16}O^{16}O + \equiv Si\text{-}^{18}O\text{-}Si \equiv . \quad (2)$$

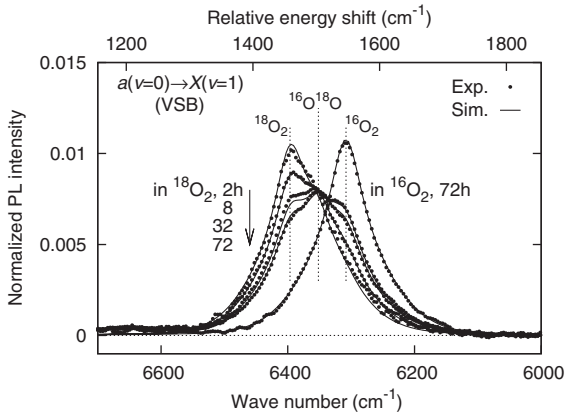

FIG. 2. Experimental and simulated VSB spectra normalized to the PEB amplitude for samples thermally annealed at 700 °C in $^{16}O_2$ or $^{18}O_2$.

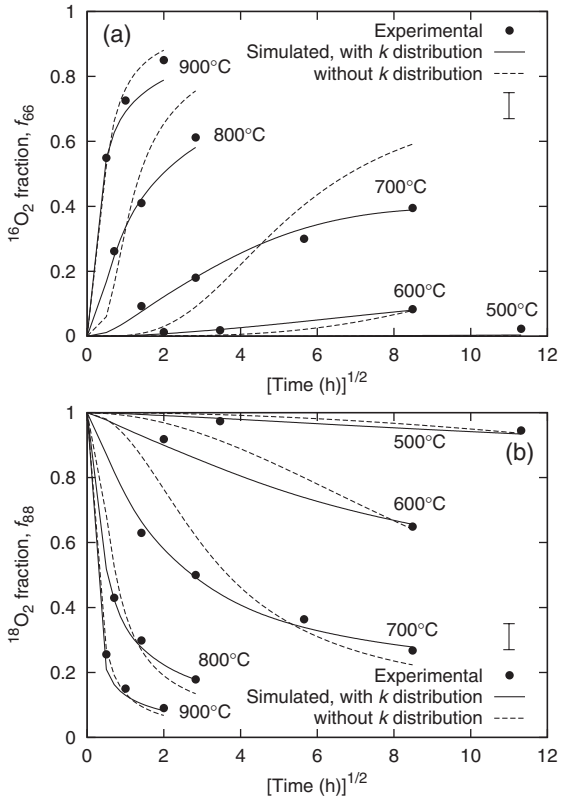

FIG. 3. Variation of the fractions of (a) interstitial $^{16}O_2$ and (b) $^{18}O_2$ (f_{66} and f_{88}, respectively) with time and temperature of the thermal annealing in $^{18}O_2$ gas. The filled symbols were derived by peak decomposition of VSB under the restriction condition $f_{66} + f_{68} + f_{88} = 1$. The solid and dashed lines were drawn by directly simulating the VSB spectra from the solutions of the rate equations Eq. (3)–(6). The simulation was performed both with and without considering the distribution in the exchange rate constant k. The error bars represent the experimental uncertainties.

We defined the exchange rate constant of Eq. (1) forward and Eq. (2) backward reactions as k. Then the rate constant of the Eq. (1) backward and Eq. (2) forward reactions apparently becomes $k/2$ as only one oxygen atom in $^{16}O^{18}O$ contributes to these reactions. k may be affected by the local configuration of the glass network, which differs from site to site due to the variation in the Si-O-Si angle and the local network topology [25,26]. We assumed that the network oxygen atoms have nonequal exchange rates k with a Gaussian probability distribution against log$k$ [27], and each k has an Arrhenius-type dependence on the absolute annealing temperature T with common preexponential rate constant. This distribution was approximated by a finite number i of components [28], each having exchange rate k_i. The concentrations of the network ^{16}O and ^{18}O atoms for the component i (N_i and N_i^*) were normalized by the total concentration as $N^T = \sum_i (N_i + N_i^*) = 4.41 \times 10^{22}$ cm^{-3} [29]. The temporal and spatial variations of interstitial $^{16}O_2$, $^{16}O^{18}O$, and $^{18}O_2$ concentrations (C, C^*, and C^{**} where $C^T = C + C^* + C^{**}$) were calculated by numerically solving following simultaneous one-dimensional diffusion-exchange equations.

$$\frac{\partial C^T}{\partial t} = D\frac{\partial^2 C^T}{\partial x^2}, \tag{3}$$

$$\frac{\partial C}{\partial t} = D\frac{\partial^2 C}{\partial x^2} + \sum_i k_i\left(\frac{C^*}{2}N_i - CN_i^*\right), \tag{4}$$

$$\frac{\partial C^{**}}{\partial t} = D\frac{\partial^2 C^{**}}{\partial x^2} + \sum_i k_i\left(-C^{**}N_i + \frac{C^*}{2}N_i^*\right), \tag{5}$$

$$\frac{\partial N_i^*}{\partial t} = -\frac{\partial N_i}{\partial t} = k_i\left(\frac{C^*}{2}N_i + C^{**}N_i - CN_i^* - \frac{C^*}{2}N_i^*\right). \tag{6}$$

VSB spectra (Fig. 2, solid lines) were calculated from the solutions and fitted to the observed spectra. A boundary condition was set as $C^T = C^{**} = 0.9ST/298$ at the sample surfaces, taking into account that (i) solubility of O_2 depends linearly on the O_2 pressure inside the silica tube [17,30], which is roughly proportional to T, (ii) dissolution of O_2 is much faster than the subsequent diffusion of interstitial O_2 [16,17], and (iii) the ^{18}O fraction of O_2 gas in the tube remained close to 1 during the thermal annealing.

As shown in Fig. 3, the solutions of the rate equations Eqs. (3)–(6) (solid lines) agreed well with the experimental variation of f_{66} and f_{88} (filled symbols) when k is distributed; it was not possible to obtain a good fit using a single k value. The full width at half maximum of the distribution of log$k$ was ~9.7 at 500 °C and ~6.4 at 900 °C, indicating that a part of network oxygen atoms are much more reactive than the remaining network oxygen atoms. These more reactive sites easily release ^{16}O and enhance the formation of interstitial $^{16}O^{18}O$ and $^{16}O_2$ in an early stage of the oxygen loading. Later in the reaction, however, such sites have been occupied by ^{18}O while the remaining sites release ^{16}O more gradually, slowing the increase in f_{66} and f_{68}.

The average exchange rate constant k_a for systems with a k distribution may be represented by the simple weighted average of k_i as $k_a = \sum_i k_i(N_i + N_i^*)/N_T$. Figure 4 shows the dependence of k_a on T, where k_a ranged from ~10^{-28} to ~10^{-23} cm^3 s^{-1} according to the change in T between 500 and 900 °C. The activation energy for k_a, which may be given by assuming a linear relation between logk_a and T^{-1}, was ~2.1 eV. Secondary ion mass spectroscopy profiling studies have reported similar values (~2.6 [12] and ~1.7 eV [13]), although they assumed first-order exchange reactions. These values are larger than the activation energy for the permeation of interstitial O_2 in a-SiO_2 (~0.8–1.2 eV [17,30,31]), suggesting that the oxygen exchange is not the bottleneck for the permeation. In contrast, they are much smaller than the energies of the O-O bond in O_2 (~5.1 eV), and Si-O bond (~4.7 eV), and the

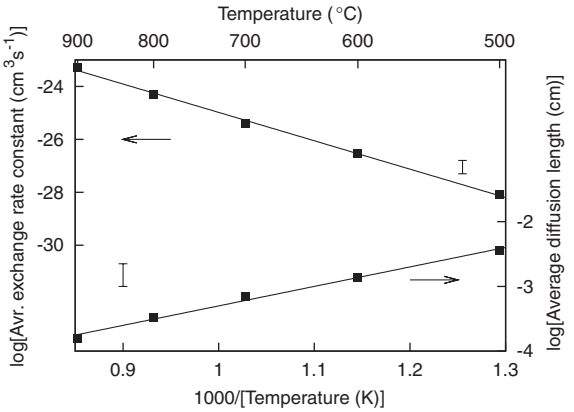

FIG. 4. Temperature dependence of the average exchange rate constant k_a and the average exchange-free diffusion length l of an interstitial O_2 molecule [Eq. (7)]. The error bars represent the experimental uncertainties.

activation energy for the viscous flow of a-SiO_2 (~5–7 eV [32–34]) that is required for network rearrangement. Thus, the observed activation energy may correspond to the energy needed to form an activation complex during the oxygen exchange.

The average time interval of the oxygen exchange for an interstitial O_2 molecule may be given by $(k_a N^T)^{-1}$, yielding $\sim 3 \times 10^5$ s at 500 °C and ~6 s at 900 °C. Using this value, the average exchange-free diffusion length l of an interstitial O_2 molecule in one dimension may be calculated by

$$l = 2\left(\frac{Dt}{\pi}\right)^{1/2} = 2\left(\frac{D}{\pi k_a N^T}\right)^{1/2}. \quad (7)$$

Calculated l values are plotted in Fig. 4; they were ~40 μm at 500 °C and ~2 μm at 900 °C, demonstrating that l is far larger than the scale of the ring and cage structures of the a-SiO_2 network (~1 nm [26,29]).

In summary, we developed a photoluminescence technique to quantitatively study ^{18}O-labeled interstitial O_2 in amorphous SiO_2, which offers a direct way to investigate their property and intrinsic reactivity. The obtained results provide insight into interactions of O_2 with oxides.

*Author to whom correspondence should be addressed: kkaji@tmu.ac.jp

[1] J. H. Lunsford, Catal. Rev. **8**, 135 (1974).
[2] A. Bielański and J. Haber, Catal. Rev. **19**, 1 (1979).
[3] M. Che and A. J. Tench, Adv. Catal. **32**, 1 (1983).
[4] H. C. Lu, T. Gustafsson, E. P. Gusev, and E. Garfunkel, Appl. Phys. Lett. **67**, 1742 (1995).
[5] M. L. Green, E. P. Gusev, and E. L. Garfunkel, J. Appl. Phys. **90**, 2057 (2001).
[6] R. Rosencher, A. Straboni, S. Rigo, and G. Amsel, Appl. Phys. Lett. **34**, 254 (1979).
[7] M. A. Lamkin, F. L. Riley, and R. J. Fordham, J. Eur. Ceram. Soc. **10**, 347 (1992).
[8] A. Bongiorno and A. Pasquarello, Phys. Rev. Lett. **88**, 125901 (2002).
[9] R. H. Doremus, J. Non-Cryst. Solids **349**, 242 (2004).
[10] K. Tatsumura, T. Shimura, E. Mishima, K. Kawamura, D. Yamasaki, H. Yamamoto, T. Watanabe, M. Umeno, and I. Ohdomari, Phys. Rev. B **72**, 045205 (2005).
[11] A. G. Revesz, B. J. Mrstik, and H. L. Hughes, J. Electrochem. Soc. **134**, 2911 (1987).
[12] J. D. Cawley and R. S. Boyce, Philos. Mag. A **58**, 589 (1988).
[13] J. D. Kalen, R. S. Boyce, and J. D. Cawley, J. Am. Ceram. Soc. **74**, 203 (1991).
[14] C. Schweitzer and R. Schmidt, Chem. Rev. **103**, 1685 (2003).
[15] L. Skuja, B. Güttler, D. Schiel, and A. R. Silin, Phys. Rev. B **58**, 14296 (1998).
[16] K. Kajihara, T. Miura, H. Kamioka, M. Hirano, L. Skuja, and H. Hosono, J. Ceram. Soc. Jpn. **112**, 559 (2004).
[17] K. Kajihara, H. Kamioka, M. Hirano, T. Miura, L. Skuja, and H. Hosono, J. Appl. Phys. **98**, 013529 (2005).
[18] K. Kajihara, T. Miura, H. Kamioka, A. Aiba, M. Uramoto, Y. Morimoto, M. Hirano, L. Skuja, and H. Hosono, J. Non-Cryst. Solids **354**, 224 (2008).
[19] R. Schmidt and E. Afshari, Ber. Bunsen-Ges. Phys. Chem. **96**, 788 (1992).
[20] K. Kajihara, S. Matsuishi, K. Hayashi, M. Hirano, and H. Hosono, J. Phys. Chem. C **111**, 14855 (2007).
[21] ^{18}O fractions recorded before and after thermal annealing were $\gtrsim 0.99$ and $\gtrsim 0.97$, respectively.
[22] K. Kajihara, H. Kamioka, M. Hirano, T. Miura, L. Skuja, and H. Hosono, J. Appl. Phys. **98**, 013528 (2005).
[23] Peak position determined by fitting with a pseudo Voigt function. The maximum is located at a bit higher energy, ~7857 cm^{-1}.
[24] R. H. Doremus, J. Electrochem. Soc. **143**, 1992 (1996).
[25] R. L. Mozzi and B. E. Warren, J. Appl. Crystallogr. **2**, 164 (1969).
[26] *Defects in* SiO_2 *and Related Dielectrics: Science and Technology*, edited by G. Pacchioni, L. Skuja, and D. L. Griscom, NATO Science Series II: Mathematics, Physics and Chemistry (Kluwer Academic Publishers, Dordrecht, Netherlands, 2000).
[27] It corresponds to the Gaussian distribution in the activation energy for k when k follows an Arrhenius-type temperature dependence.
[28] We set $|i| \leqq 15$ and confirmed that further increase in $|i|$ does not influence the results.
[29] R. H. Doremus, *Diffusion of Reactive Molecules in Solids and Melts* (John Wiley & Sons, New York, 2002).
[30] F. J. Norton, Nature (London) **191**, 701 (1961).
[31] C. C. Tournour and J. E. Shelby, Phys. Chem. Glasses **46**, 559 (2005).
[32] G. Hetherington, K. H. Jack, and J. C. Kennedy, Phys. Chem. Glasses **5**, 130 (1964).
[33] R. H. Doremus, J. Appl. Phys. **92**, 7619 (2002).
[34] H. Kakiuchida, K. Saito, and A. J. Ikushima, J. Appl. Phys. **93**, 777 (2003).